PAPER

Check for updates

The synthesis of competing phase GeSe and GeSe₂ 2D layered materials

Kentaro Yumigeta, Cassondra Brayfield, [ID] Hui Cai, Debarati Hajra, Mark Blei, Sijie Yang, Yuxia Shen and S. Tongay [ID] *

We demonstrate the synthesis of layered anisotropic semiconductor GeSe and GeSe₂ nanomaterials through low temperature (~400 °C) and atmospheric pressure chemical vapor deposition using halide based precursors. Results show that GeI_2 and H_2Se precursors successfully react in the gas-phase and nucleate on a variety of target substrates including sapphire, Ge, GaAs, or HOPG. Layer-by-layer growth takes place after nucleation to form layered anisotropic materials. Detailed SEM, EDS, XRD, and Raman spectroscopy measurements together with systematic CVD studies reveal that the substrate temperature, selenium partial pressure, and the substrate type ultimately dictate the resulting stoichiometry and phase of these materials. Results from this work introduce the phase control of Ge and Se based nanomaterials (GeSe and GeSe₂) using halide based CVD precursors at ATM pressures and low temperatures. Overall findings also extend our fundamental understanding of their growth by making the first attempt to correlate growth parameters to resulting competing phases of Ge–Se based materials.

Introduction

Two-dimensional (2D) materials are atomically thin material systems with extraordinary optical, electrical, thermal, and magnetic properties.[1,2] Post-transition metal mono-chalcogenide (PTMCs) materials are members of this large 2D materials family and have the general chemical formula of MX[3,4] wherein M stands for metals from groups IIIA and IVA (In, Ga, Ge, Sn) and X is VIA chalcogenides (S, Se, and Te). These material systems have shown unique properties that are vastly different from other 2D systems such as dichalcogenides or trichalcogenides.[3,5] Because of small exciton binding energies (~10–20 meV) and indirect gap from bulk to monolayers, they are potential photovoltaic materials with efficient e–h generation and separation characteristics. They have been proposed as active semiconductors for water splitting applications owing to their favorable band alignment characteristics with respect to reduction and oxidization energies.[6] Recently, GeSe, GeTe, SnSe, and their ternary alloys have been shown to be highly efficient new-class of phase change materials and world record *ZT* values were also reported on SnSe from PTMCs family.[7]

While germanium based van der Waals (vdW) crystals have been synthesized in the past using the modified Bridgman-Stockberger method,[8] it was only until recently GeSe and GeS bulk crystals have been commercialized. The synthesis

Materials Science and Engineering, School for Engineering of Matter, Transport and Energy, Arizona State University, Tempe, AZ 85287, USA. E-mail: sefaattin.tongay@asu.edu

procedures and protocols for bulk GeSe₂ vdW crystal – another layered phase in the Ge–Se diagram – is still lacking. Despite their potential, the synthesis of ultrathin GeSe₂ is still at its seminal stages and experimental studies rely on exfoliation.[9] GeSe₂ synthesis by CVD using GeI_4 and Se has been reported.[10] Recently, Hu *et al.* have synthesized GeSe by salt-assisted CVD using GeSe₂ precursor.[11] However, reported GeSe synthesis by CVD is limited and the method to control the phase of Ge–Se system during CVD is unknown. 2D or ultra-thin Ge based layered materials are commercially still not available due to a fundamental knowledge gap in synthesis of these materials.

Here for the first time, we report GeI_2 and Se precursor based chemical vapor deposition technique (CVD) for depositing GeSe and GeSe₂ ultrathin nanomaterials onto a variety of substrates. Our systematic studies show that the technique relies on the high temperature reaction of H_2Se vapor with GeI_2 in close proximity to other substrates. When these two precursors react, CVD growth produces either GeSe or GeSe₂ depending on the substrate type, target temperature, and Se partial pressure. Both materials crystallize in their layered form and their composition as well as the crystal structures can be controlled by careful thermal profiling depending on the substrate type and overall growth temperature. This process takes place at low temperature (~400 °C) which is essential to its compatibility with the semiconductor industry. Raman spectroscopy, energy dispersive X-ray spectroscopy (EDS), scanning electron microscopy (SEM), angle resolved Raman spectroscopy (ARS), and our CVD technique establish the first ever growth of GeSe by halide based precursor and the phase control between GeSe and GeSe₂.

Chemical vapor deposition of GeSe and GeSe$_2$

The proposed technique relies on the reaction of GeI$_2$ and Se in close proximity to target substrates as shown in Fig. 1. In this process, GeI$_2$ and Se precursors were selected mainly because of their low melting points, high vapor pressures and chemical reactivities. Selenium powder melts at 220 °C and GeI$_2$ sublimes at 240 °C. In order to reach sufficient and similar vapor Se and Ge pressures, we have placed our GeI$_2$ at the center of the 1 inch diameter single zone furnace and kept at ~500 °C, while Se powder was approximately at 11–15 cm from GeI$_2$ at 410–460 °C. Here, Se precursor temperature was systematically varied by changing the position of the Se powder (Fig. 1a). The temperature profiling (Fig. 1b) shows the locations of Se, GeI$_2$, and substrates and their keep temperatures, respectively. For simplicity, we denote the Se precursor temperature as T_{Se}, the GeI$_2$ precursor temperature as T_{GeI2} and the substrate temperature as T_g. In a typical growth, we have used 40 mg of Se powder (99.999%, Sigma-Aldrich) and 40 mg of GeI$_2$ powder (99.999%, Alfa Aesar). These powders were placed on two quartz boats and 3 standard cubic centimeters per minute (sccm) of Ar and 7 sccm of H$_2$ were used as carrier gas at atmospheric pressure. In our study, substrates were selected from Ge (100) (University wafer), GaAs (100) (American Xtal Technology), c-cut sapphire (Ckplas), Highly oriented pyrolytic graphite (HOPG) (Materials Quartz).

Growth and the effect of the substrate

Synthesis was carried out using a variety of different substrates such as germanium, GaAs, sapphire, and graphite vdW surfaces (Fig. 1a and b). Typical growth at $T_g = 420$ °C using germanium substrates produced rectangular phased GeSe ultra-thin materials which measures tens of microns in lateral sizes.

Comparison between Raman spectroscopy data collected from Bridgman grown GeSe crystals and GeSe films show that material crystalizes in alpha-phase GeSe (Fig. 2b). The full width at half maximum (FWHM) of the Raman spectrum from CVD-grown GeSe (4.8 cm^{-1}) is much sharper compared to FWHM of Bridgman grown GeSe crystal (6.3 cm^{-1}) highlighting the crystallinity of the as-grown GeSe sheets. Energy-dispersive X-ray spectroscopy (EDS) measurements on CVD grown GeSe also confirm the stoichiometry of the synthesized layers (Fig. 2c).

In order to determine the crystallinity and the degree of anisotropy (measure of crystalline anisotropy of the crystal), we have further performed angle resolved Raman spectroscopy measurements as shown in Fig. 2h. Previously, this method has been used for other 2D anisotropic material systems to provide a fast, quick, noncontact optical method to determine the crystalline orientation.[12–17] In this method, Raman intensity of an individual mode is plotted with respect to the laser polarization angle as shown in Fig. 2h. Here, the polarization angle is defined as zero 0° when the laser polarization vector is parallel along the longer edge (large-aspect ratio). B_{3g}^1 mode at 153 cm^{-1} as well as A_g^1 mode at 190 cm^{-1} display four-fold symmetry associated with their Raman tensor characteristics, and thus cannot be used to determine the crystal orientation of GeSe. In contrast, A_g^2 mode and A_g^3 show two-fold symmetry which are suitable to determine the crystal orientation using optical techniques. A_g^2 and A_g^3 mode Raman mode intensity maximizes when the polarization vector angle is ~90° and ~0°, respectively. Overall 2-lobed features demonstrate that synthesized GeSe sheets are highly crystalline and have good anisotropy. We note however that the full coverage growth is rather challenging since the nucleation density is small and the lateral growth speed is slow.
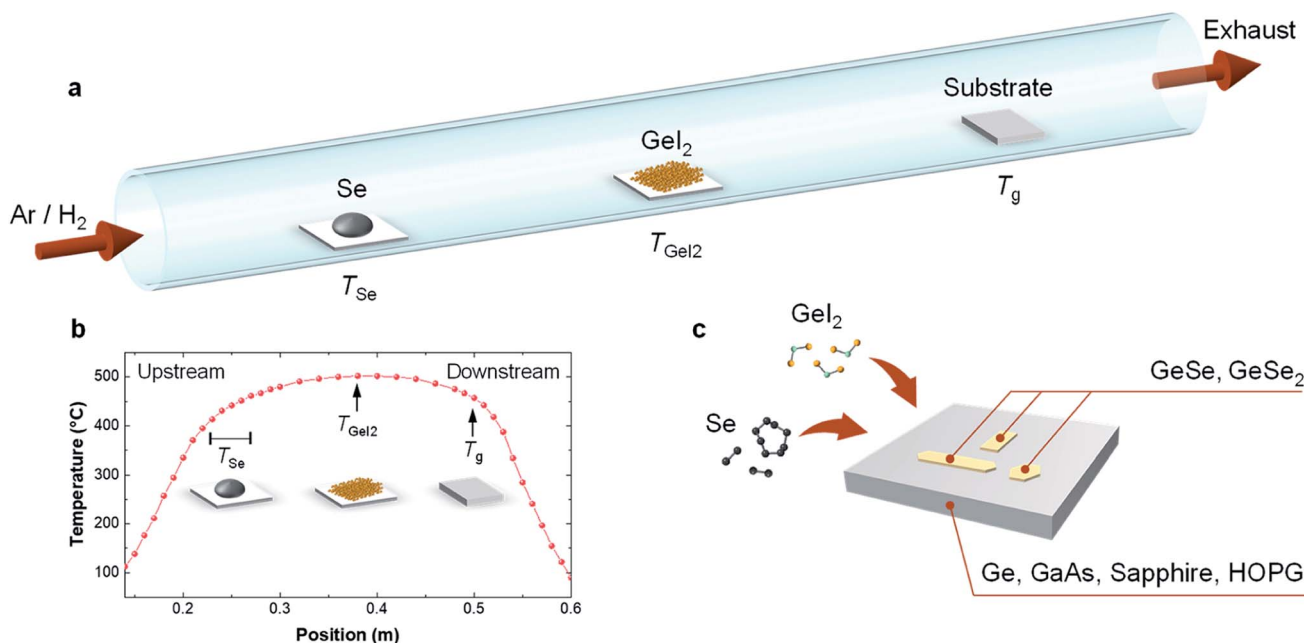

Fig. 1 (a) Schematic diagram of the CVD growth of GeSe and GeSe$_2$ ultrathin layers. (b) Temperature profile of the furnace and the position of precursors in relation to the target substrate. (c) Schematic description of GeSe and GeSe$_2$ formation process on various substrates.
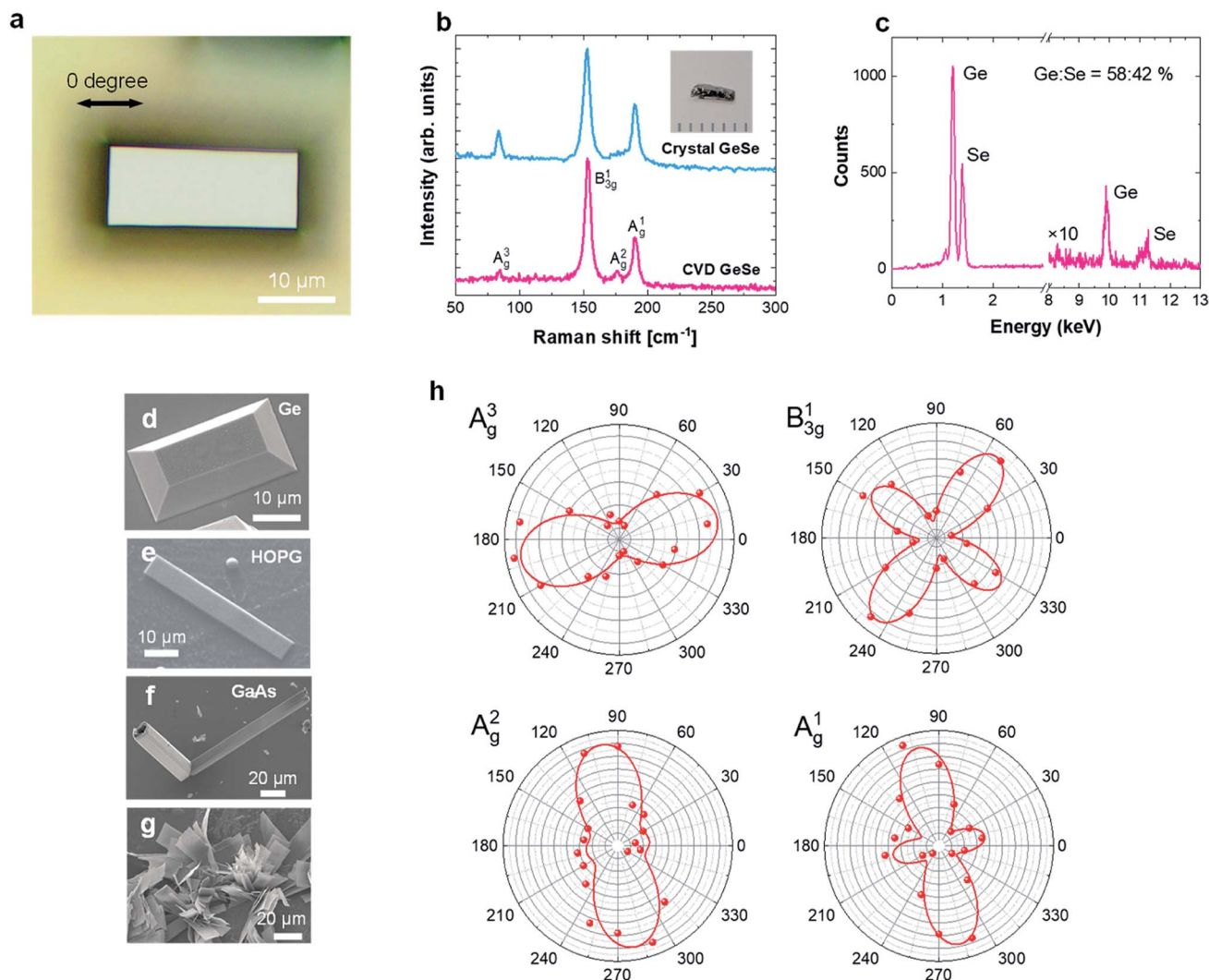
Fig. 2 (a) Optical image of CVD-grown GeSe. (b) Comparison between the Raman spectra of bulk GeSe crystal and CVD-grown GeSe. (c) EDS spectrum of CVD-grown GeSe. (d–f). SEM image of GeSe on various substrates. (g) SEM images from flower-like lamellar GeSe sheets. (h) Angle resolved Raman spectra contour plots shown for different Raman modes.

From the optical and SEM images, we find that the surface type and characteristics play a significant role in the type of growth mode. For example, truncated rectangular pyramidal crystals shown in Fig. 2d are attained on single crystal germanium substrates, while flat thin GeSe sheets form on HOPG surfaces (Fig. 2e). On the other hand, the sheets grown on GaAs substrate have out of the plane growth similar to flower like features as shown in Fig. 2f. This might be related to the fact that the elastic energy of GeSe on the substrates is 0.032 meV on Ge(100), 0.046 meV on GaAs. This higher elastic energy on GaAs may promote out-of-plane growth of GeSe.[18] In contrast, the elastic energy of HOPG is small since the substrate is a known van der Waals material and may promote layer-by-layer growth. Here, we note that when the flow rate is much higher (Ar at 20 sccm, H_2 at 50 sccm), the growth speed increases dramatically and the system deviates from layer-by-layer growth mode resulting in similar flower-like features on other substrates as well (Fig. 2g).

Competition between GeSe and GeSe$_2$ and phase control

In our studies, we have found that the crystal shape on GaAs substrate varies with changing T_{Se} (Fig. 3a). Quasi-1D ribbons grew at $T_{Se} = 410$ and 430 °C whereas GeSe$_2$ are observed above $T_{Se} = 440$ °C, however, the shape was elongated hexagonal at 440 °C and ribbon-like at 460 °C. We have confirmed that the stoichiometry of the grown ultrathin sheets are $\sim$1 : 1 for T_{Se} < 430 °C and $\sim$1 : 1.6 for T_{Se} > 430 °C by EDS measurement (Fig. 3b). We further confirmed by Raman spectroscopy that the crystals for T_{Se} < 430 °C shows GeSe spectrum while for T_{Se} > 430 °C shows GeSe$_2$ (Fig. 3c) which marks the first synthesis of GeSe$_2$ nanosheets. In the phase diagram of germanium selenide (Fig. 3d), GeSe$_2$ grows at higher temperatures compared to GeSe. Our studies, however, show that GeSe and GeSe$_2$ ultrathin sheets can be grown at the same temperature by simply changing the Se partial pressure (Fig. 3a and e). It is also noteworthy that the temperature ranges show significant differences in our CVD process compared to established bulk
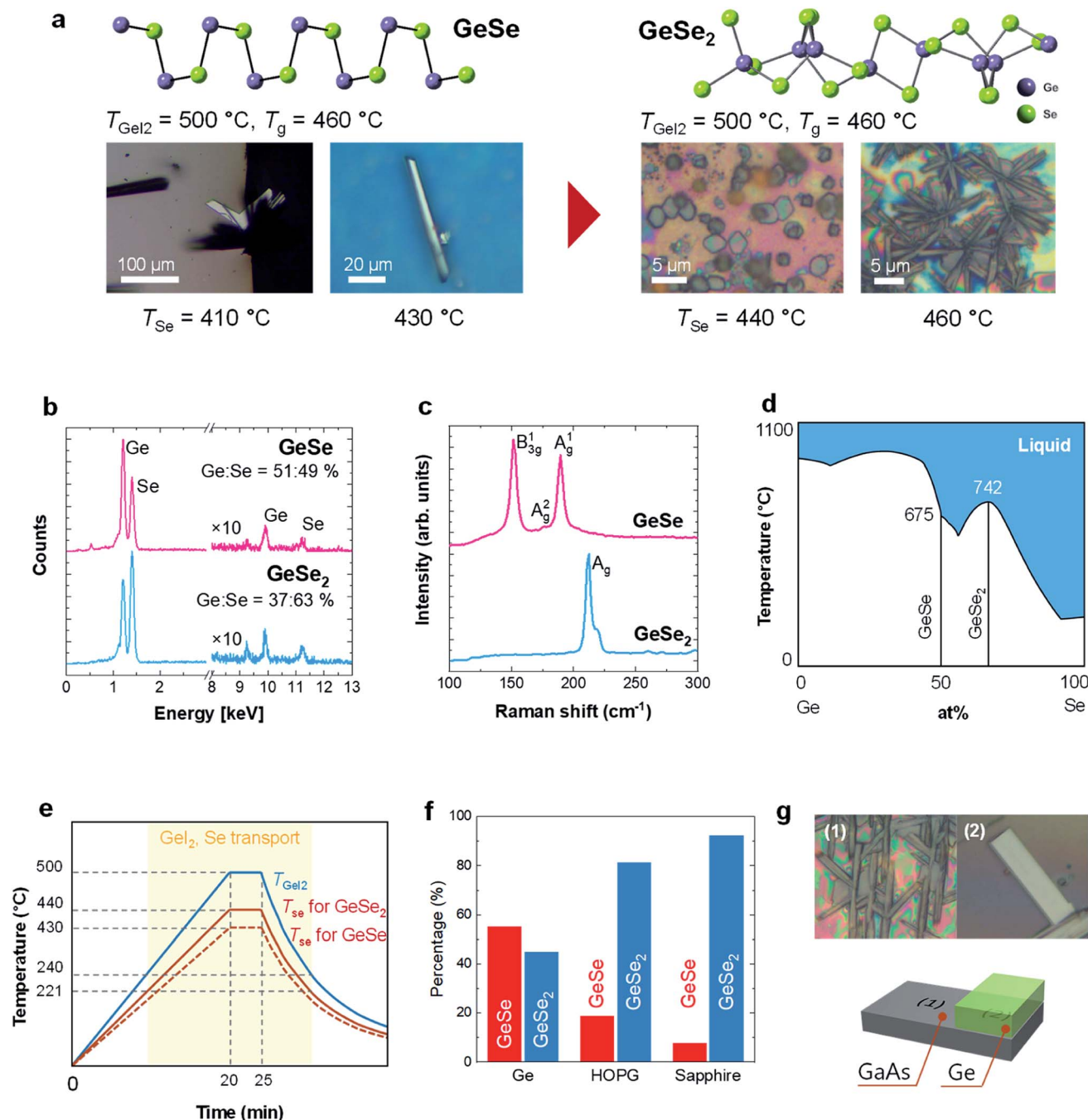
Fig. 3 (a) Crystal structures and optical image of grown GeSe and GeSe$_2$. GeSe grows at lower T_{Se} while GeSe$_2$ grows at higher T_{Se}. T_{GeI_2} and T_g are fixed. (b) Raman spectra and (c) EDS spectra of GeSe and GeSe$_2$ on GaAs. (d) Phase diagram of Ge−Se binary system. (e) Temperature profile of CVD growth. (f) Substrate dependence of the percentage of GeSe $vs.$ GeSe$_2$ coverage on different substrates when T_{GeI_2} and T_g are fixed but T_{Se} is varied. (g) Crystals on GaAs (c.1) without and (c.2) with Ge substrate capping.

phase diagrams[19] which can be attributed to the fact that phase diagrams deviate significantly going from bulk to nano-materials due to differences in surface to volume ratio. Even though GeSe and GeSe$_2$ call for different growth temperatures, our process enables a GeSe to GeSe$_2$ phase transition by increasing the Se concentration without changing the substrate temperature.

Raman spectroscopy measurements on the synthesized GeSe$_2$ sheets show that the Raman finger-prints closely match β phase GeSe$_2$ spectra (Fig. 4b)[20,21] and the SEM EDS elemental spectra shows that the stoichiometry of these crystals are very close to 1 : 1.8 (Fig. 4c). To determine the crystallinity and the anisotropy of GeSe$_2$ crystal, we have collected angle resolved Raman spectrum. The Raman intensity of each mode is plotted with respect to the laser polarization angle in Fig. 4d and e.
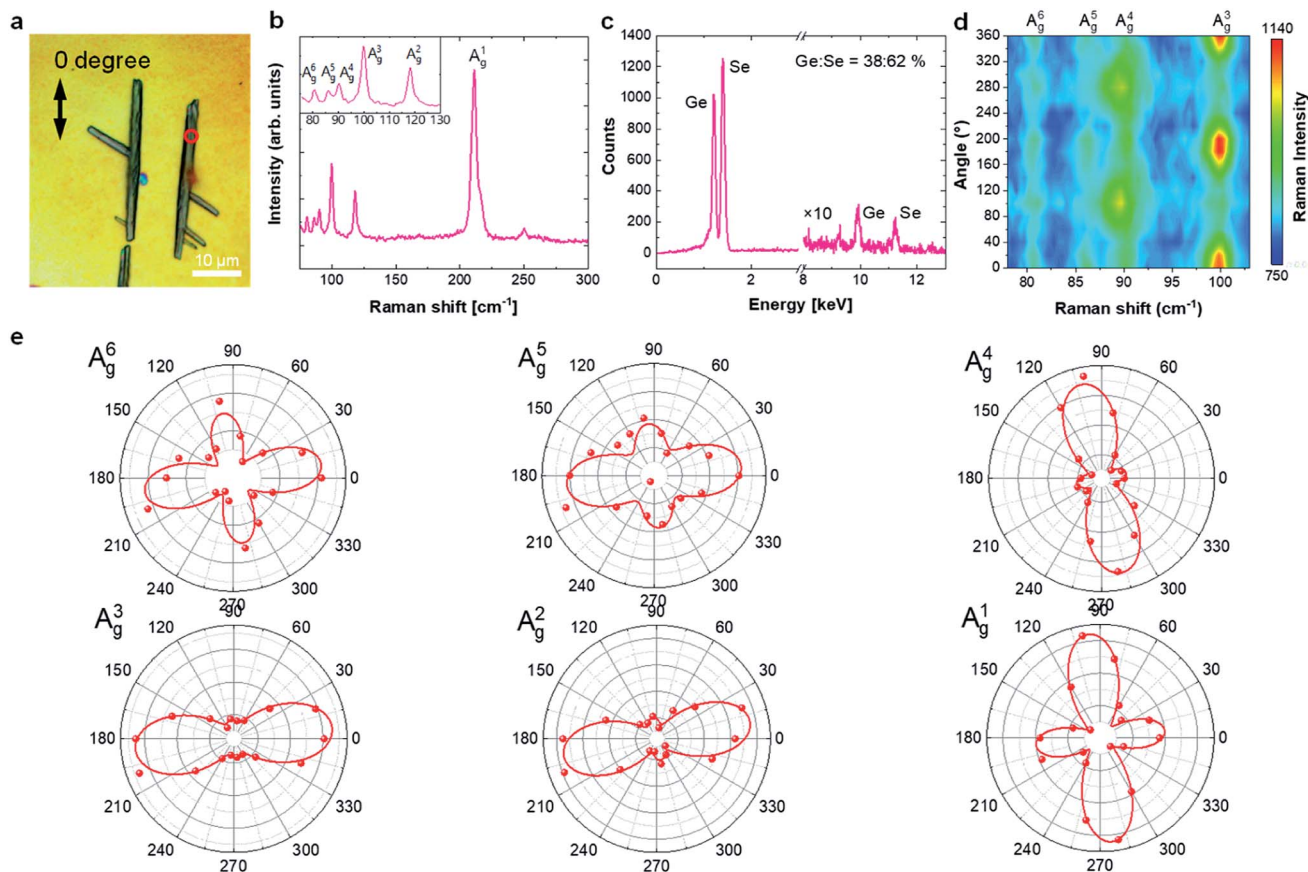
Fig. 4   (a) Optical image of $GeSe_2$. (b) Raman spectrum of $GeSe_2$. Inset shows the magnified spectrum of Raman modes. (c) EDS spectrum of $GeSe_2$. (d) Angle resolved Raman spectra and (e) contour plots for fundamental Raman modes (A_g^6, A_g^5, A_g^4, A_g^3) for $GeSe_2$.

Overall, A_g^1 mode at 211 cm^{-1}, A_g^5 mode at 86 cm^{-1} and A_g^6 mode at 80 cm^{-1} shows four-fold symmetry. On the other hand, A_g^2 mode at 118 cm^{-1}, A_g^3 mode at 100 cm^{-1} and A_g^4 mode at 90 cm^{-1} shows two-fold symmetry which can be used to determine the crystal orientation. The Raman intensity of A_g^2 mode and A_g^3 mode is strong when the laser polarization is along with the ribbon while A_g^4 becomes minimum. Further study is much needed to understand the polarization response of these prominent Raman modes in $GeSe_2$ nanosheets.

Conclusion

Here, we have reported on a new halide precursor based chemical vapor deposition technique to synthesize GeSe and the method to control two competing phases of GeSe and $GeSe_2$ based nanosheets onto different temperatures. The growth takes place at atmospheric pressure and at room temperature which is attractive for scalability considerations. Interestingly, our process enables us to synthesize both GeSe and $GeSe_2$ by simply adjusting the Se partial pressure without the need to change the substrate temperature which is generally needed for other material systems with different temperature growth windows. Established low temperature and atmospheric pressure growth process extends the fundamental knowledge of bottom-up growth for vdW layered material systems.

Conflicts of interest

There are no conflicts of interest declared.

Acknowledgements

References

1   Q. H. Wang, K. Kalantar-Zadeh, A. Kis, J. N. Coleman and M. S. Strano, Electronics and optoelectronics of two-dimensional transition metal dichalcogenides, *Nat. Nanotechnol.*, 2012, 7(11), 699–712.

2   M. Tran, K. Kline, Y. Qin, Y. Shen, M. D. Green and S. Tongay, 2D coordination polymers: design guidelines and materials perspective, *Appl. Phys. Rev.*, 2019, 6(4), 041311.

3   L. Xu, M. Yang, S. J. Wang and Y. P. Feng, Electronic and optical properties of the monolayer group-IV monochalcogenides MX (M = Ge, Sn; X = S, Se, Te), *Phys. Rev. B*, 2017, 95(23), 235434.

4 H. Cai, B. Chen, M. Blei, S. L. Y. Chang, K. Wu, H. Zhuang and S. Tongay, Abnormal band bowing effects in phase instability crossover region of GaSe1-xTe x nanomaterials, *Nat. Commun.*, 2018, **9**(1), 1927.

5 D. T. Do, S. D. Mahanti and C. W. Lai, Spin splitting in 2D monochalcogenide semiconductors, *Sci. Rep.*, 2015, **5**, 17044.

6 H. L. Zhuang and R. G. Hennig, Single-Layer Group-III Monochalcogenide Photocatalysts for Water Splitting, *Chem. Mater.*, 2013, **25**(15), 3232–3238.

7 C. Chang, M. H. Wu, D. S. He, Y. L. Pei, C. F. Wu, X. F. Wu, H. L. Yu, F. Y. Zhu, K. D. Wang, Y. Chen, L. Huang, J. F. Li, J. Q. He and L. D. Zhao, 3D charge and 2D phonon transports leading to high out-of-plane ZT in n-type SnSe crystals, *Science*, 2018, **360**(6390), 778–782.

8 V. L. Cardetta, A. M. Mancini and A. Rizzo, Melt growth of single crystal ingots of GaSe by Bridgman-Stockbarger's method, *J. Cryst. Growth*, 1972, **16**(2), 183–185.

9 Y. Yang, S.-C. Liu, W. Yang, Z. Li, Y. Wang, X. Wang, S. Zhang, Y. Zhang, M. Long, G. Zhang, D.-J. Xue, J.-S. Hu and L.-J. Wan, Air-Stable In-Plane Anisotropic GeSe₂ for Highly Polarization-Sensitive Photodetection in Short Wave Region, *J. Am. Chem. Soc.*, 2018, **140**(11), 4150–4156.

10 X. Zhou, X. Hu, S. Zhou, Q. Zhang, H. Li and T. Zhai, Ultrathin 2D GeSe₂ Rhombic Flakes with High Anisotropy Realized by van der Waals Epitaxy, *Adv. Funct. Mater.*, 2017, **27**, 1703858.

11 X. Hu, P. Huang, K. Liu, B. Jin, X. Zhang, X. Zhang, X. Zhou and T. Zhai, Salt-Assisted Growth of Ultrathin GeSe Rectangular Flakes for Phototransistors with Ultrahigh Responsivity, *ACS Appl. Mater. Interfaces*, 2019, **11**, 23353–23360.

12 W. Kong, C. Bacaksiz, B. Chen, K. Wu, M. Blei, X. Fan, Y. Shen, H. Sahin, D. Wright, D. S. Narang and S. Tongay, Angle resolved vibrational properties of anisotropic transition metal trichalcogenide nanosheets, *Nanoscale*, 2017, **9**(12), 4175–4182.

13 R. Beams, L. G. Cançado, S. Krylyuk, I. Kalish, B. Kalanyan, A. K. Singh, K. Choudhary, A. Bruma, P. M. Vora, F. Tavazza, A. V. Davydov and S. J. Stranick, Characterization of Few-Layer 1T′ MoTe₂ by Polarization-Resolved Second Harmonic Generation and Raman Scattering, *ACS Nano*, 2016, **10**(10), 9626–9636.

14 G. Wang, E. Palleau, T. Amand, S. Tongay, X. Marie and B. Urbaszek, Polarization and time-resolved photoluminescence spectroscopy of excitons in MoSe₂ monolayers, *Appl. Phys. Lett.*, 2015, **106**(11), 112101.

15 O. B. Aslan, D. A. Chenet, A. M. van der Zande, J. C. Hone and T. F. Heinz, Linearly Polarized Excitons in Single- and Few-Layer ReS₂ Crystals, *ACS Photonics*, 2016, **3**(1), 96–101.

16 K. Wu, B. Chen, S. Yang, G. Wang, W. Kong, H. Cai, T. Aoki, E. Soignard, X. Marie, A. Yano, A. Suslu, B. Urbaszek and S. Tongay, Domain Architectures and Grain Boundaries in Chemical Vapor Deposited Highly Anisotropic ReS₂ Monolayer Films, *Nano Lett.*, 2016, **16**(9), 5888–5894.

17 W. Wen, Y. Zhu, X. Liu, H. P. Hsu, Z. Fei, Y. Chen, X. Wang, M. Zhang, K. H. Lin, F. S. Huang, Y. P. Wang, Y. S. Huang, C. H. Ho, P. H. Tan, C. Jin and L. Xie, Anisotropic Spectroscopy and Electrical Properties of 2D ReS$_{2(1-x)}$Se$_{2x}$ Alloys with Distorted 1T Structure, *Small*, 2017, **13**(12), 1603788.

18 H. Ding, S. S. Dwaraknath, L. Garten, P. Ndione, D. Ginley and K. A. Persson, Computational Approach for Epitaxial Polymorph Stabilization through Substrate Selection, *ACS Appl. Mater. Interfaces*, 2016, **8**(20), 13086–13093.

19 H. Okamoto, Ge–Se (germanium–selenium), *J. Phase Equilib. Diffus.*, 2000, **20**(1), 313.

20 K. Inoue, O. Matsuda and K. Murase, Raman-Spectra of Tetrahedral Vibrations in Crystalline Germanium Dichalcogenides, GeS₂ and GeSe₂, in High and Low-Temperature Forms, *Solid State Commun.*, 1991, **79**(11), 905–910.

21 X. Zhou, X. Hu, S. Zhou, Q. Zhang, H. Li and T. Zhai, Ultrathin 2D GeSe₂ Rhombic Flakes with High Anisotropy Realized by Van der Waals Epitaxy, *Adv. Funct. Mater.*, 2017, **27**(47), 1703858.